Functional controls on monticule height and spacing in Permian stenolaemate bryozoans

Marcus M. Key, Jr.[1] [ID], Eckart Håkansson[2] and Benjamin R. Edwards[1]

[1]Department of Geosciences, Dickinson College, 28 North College Street, Carlisle, Pennsylvania, 17013 USA;
[2]School of Earth Sciences, University of Western Australia, 35 Stirling Highway, Crawley WA 6009, Australia

Abstract

One of the challenges for bryozoans is to avoid refiltering water that has already had its plankton removed. Larger colonies develop colony-wide maculae-centered feeding currents to avoid refiltering water and generally have elevated maculae (monticules). We hypothesize that the height and density of spacing of monticules are inversely proportional to curvature of the colony surface. Larger, flatter colonies should have higher and more closely spaced monticules. We compare two Permian stenolaemate bryozoans whose colonies form branches with elliptical cross sections: the smaller and more elliptical cystoporate *Evactinostella crucialis* (Hudleston, 1883) from Western Australia (N = 17) and the larger and flatter trepostome *Tabulipora* sp. from eastern North Greenland (N = 15). Using calipers and digital elevation models, we measured curvature, monticule height, and number of monticules per area. Results indicate that *Evactinostella* branches are at least twice as curved as those of *Tabulipora*, their monticules are half the height of *Tabulipora*, and their monticules are 22% less densely spaced than those of *Tabulipora*. In *Evactinostella* colonies, surface curvature is inversely proportional to monticule height and spatial density, which is not true for *Tabulipora*. Therefore, we conclude that the smaller and more curved the colony surface, the less the colony needs robust colony-wide feeding currents created by tall, closely spaced monticules.

Non-technical Summary

Bryozoans (also known as colonial moss animals) filter plankton from ocean water for their food. They struggle with refiltering the same water repeatedly. They have evolved bumps on their colony surfaces to solve this problem. We think the height and spacing of these bumps should be inversely proportional to how curved the colony surface is. We test this idea using 285 million year old fossil bryozoans from Greenland and Australia. We show that the bumps are larger and closer on less-curved colonies as we predicted.

Introduction

One of the challenges for filter feeding animals is how to maximize feeding by minimizing refiltering previously filtered water (Hentschel and Shimeta, 2008). This is less of a problem for motile filter feeders (e.g., whale sharks or flamingos; Colman, 1997; Anderson, 2017) than for sessile ones. Bryozoans are sessile filter feeders whose ciliated tentacles of their lophophore create a feeding current that draws plankton toward their mouth (Pratt, 2004, fig. 2; Winston and Migotto, 2021, fig. 6.4). This creates two problems for bryozoans. First, the filtered water accumulates between the canopy of tentacles and the colony surface causing a pressure buildup that stifles feeding (Shunatova and Ostrovsky, 2002, figs. 4, 5). Second, previously filtered water gets refiltered in eddies (Grünbaum, 1995, fig. 6a; Pratt, 2004, fig. 7A(i)). Bryozoans overcome this problem by creating colony-wide feeding currents that keep the incurrent unfiltered water separate from the excurrent of previously filtered water, thus reducing refiltering of water and improving feeding efficiency (Banta et al., 1974; Cook, 1977; Winston, 1978, 1979; Taylor, 1979; Lidgard, 1981; Dick, 1987; Eckman and Okamura, 1998; Pratt, 2004; von Dassow, 2005a). The same phenomenon has also evolved in sponges (Bidder, 1923) and colonial ascidians (Vogel, 1994).

Empirical data and mathematical modeling of water flow in encrusting bryozoan colonies have shown that currents created by individual zooids may interact deleteriously (Bishop and Bahr, 1973; Thorpe and Ryland, 1987; Grünbaum, 1995). This suggests colony-wide feeding currents are beneficial to the colony at least in low current velocities where flow remains laminar (Grünbaum, 1997; Eckman and Okamura, 1998). The filtered water typically flows between the canopy of tentacles and the colony surface toward macular chimneys through which the previously filtered water is ejected away from the colony surface (McKinney, 1986a, fig. 4A; Taylor, 1999, fig. 41.3; Okamura and Partridge, 2009, fig. 3). Macular chimneys typically form on flat or more often elevated parts of a colony called monticules (Banta et al., 1974, fig. 1; Winston, 2010, fig. 2).

CAMBRIDGE
UNIVERSITY PRESS

The bigger and flatter the colony surface, the greater the problem with refiltering water due to the greater incurrent volume (McKinney, 1986a, b). McKinney (1986b) showed that in cylindrical colonies, macular chimneys form only in branches >2 mm diameter. That is because the surfaces of smaller-diameter cylinders are curved enough that the previously filtered water can escape between the lophophores. Larger-diameter cylinders have less surface curvature (Fig. 1). That is why the surface of our large spherical planet seems flat when standing on it. Branches on the largest bryozoan colonies are not cylindrical but frondose (Cuffey and Fine, 2006). Frondose branches are typically more elliptical in cross section, for example, *Heterotrypa frondosa* (d'Orbigny, 1850). Curvature varies across a frondose branch unlike a cylindrical branch.

Mathematics of curvature. In cylindrical branches, the transverse section is a circle, so all the radii are equal. In frondose branches, the transverse section is an ellipse with two axes of unequal lengths. The equation for an ellipse is

$$\frac{x^2}{a^2} + \frac{y^2}{b^2} = 1 \qquad (1)$$

where x and y are coordinates (x, y) of any point on the ellipse, and a is the length of the semi-major axis, and b is the length of the semi-minor axis (Fig. 2).

One measures the "flatness" of the surface of an ellipse by its curvature (K) (Lebedeva et al., 2015: p. 91, eq. 9).

$$/K/ = \frac{a^4 b}{\left(a^4 + x^2(b^2 - a^2)\right)^{3/2}} \qquad (2)$$

If we measure curvature at top center of the ellipse at point (x, y), then (x, y) becomes $(0, b)$ and curvature reduces to:

$$/K/ = \frac{b}{a^2} \qquad (3)$$

As a result, curvature across an elliptical branch decreases with increasing eccentricity (Fig. 3).
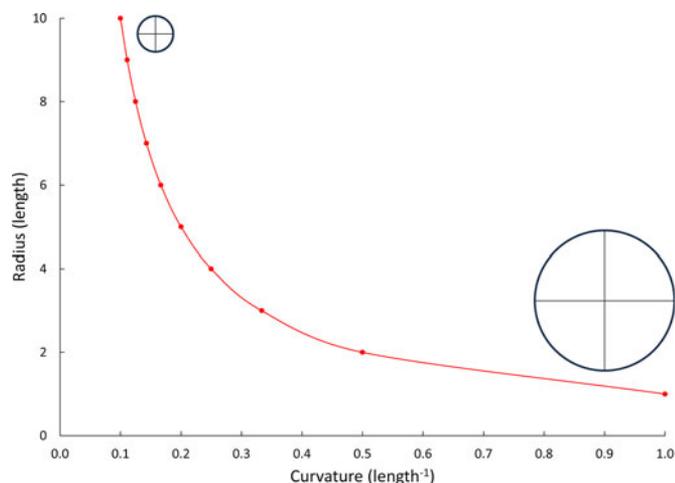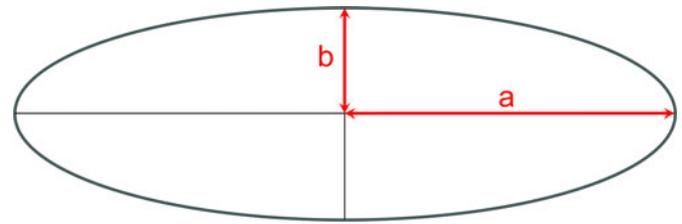

Figure 2. Geometry of an ellipse showing the semi-major (a) and semi-minor (b) axes.

The goal of this study is to see how branch surface curvature affects monticule height and spacing using two Permian stenolaemate bryozoans, both with blade-like monticulate branches with varying cross-sectional shape and size. Our hypothesis is that the curvature of the colony surface is inversely proportional to both the height and spatial density of monticules.

Materials and geologic setting

This study is based on colonies of two species of Permian stenolaemate bryozoans. *Evactinostella crucialis* (Hudleston, 1883) is a cystoporate stenolaemate bryozoan (Yancey et al., 2019). This species forms erect four-vaned colonies (Håkansson et al., 2016). The bifoliate vertical vanes are very elliptical in cross section, up to 1 cm thick, less than 10 cm wide, with heights reaching more than 25 cm (Crockford, 1957). For this study, 17 colonies of *E. crucialis* were selected from Cisuralian strata in the East Gondwana Rift Zone in Western Australia. Of these, four specimens were selected from the Jimba Jimba Member of the Callytharra Formation exposed northwest of Jimba Jimba Station at 25.0239°S, 115.0717°E, and 13 colonies were selected from the Callytharra Formation exposed in the Lyndon River gully at 23.8600°S, 114.4792°E (Fig. 4). Both sections are in the Merlingleigh Subbasin at the southern end of the onshore Southern Carnarvon Basin, Western Australia (Haig et al., 2014) (Fig. 5). Specimen numbers and collection information are available in Table 1. Stratigraphically following the International Chronostratigraphic Chart v2023/09, these colonies lived during the Artinskian Age of the Cisuralian Epoch of the Permian Period (Haig et al., 2014; Henderson et al., 2020).

Figure 1. Geometric relationship between cylinder radius and curvature of the cylinder's surface. Insets show transverse sections through endmember cylindrical branches.
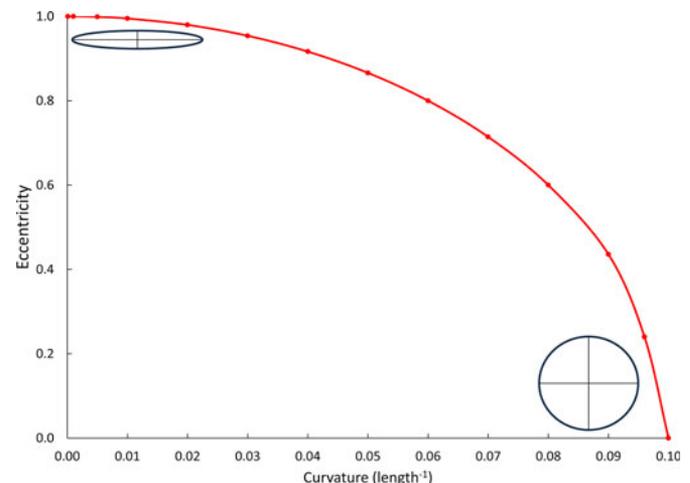

Figure 3. Graph showing how curvature across an elliptical branch decreases with increasing eccentricity. Insets show transverse sections through endmember elliptical branches.
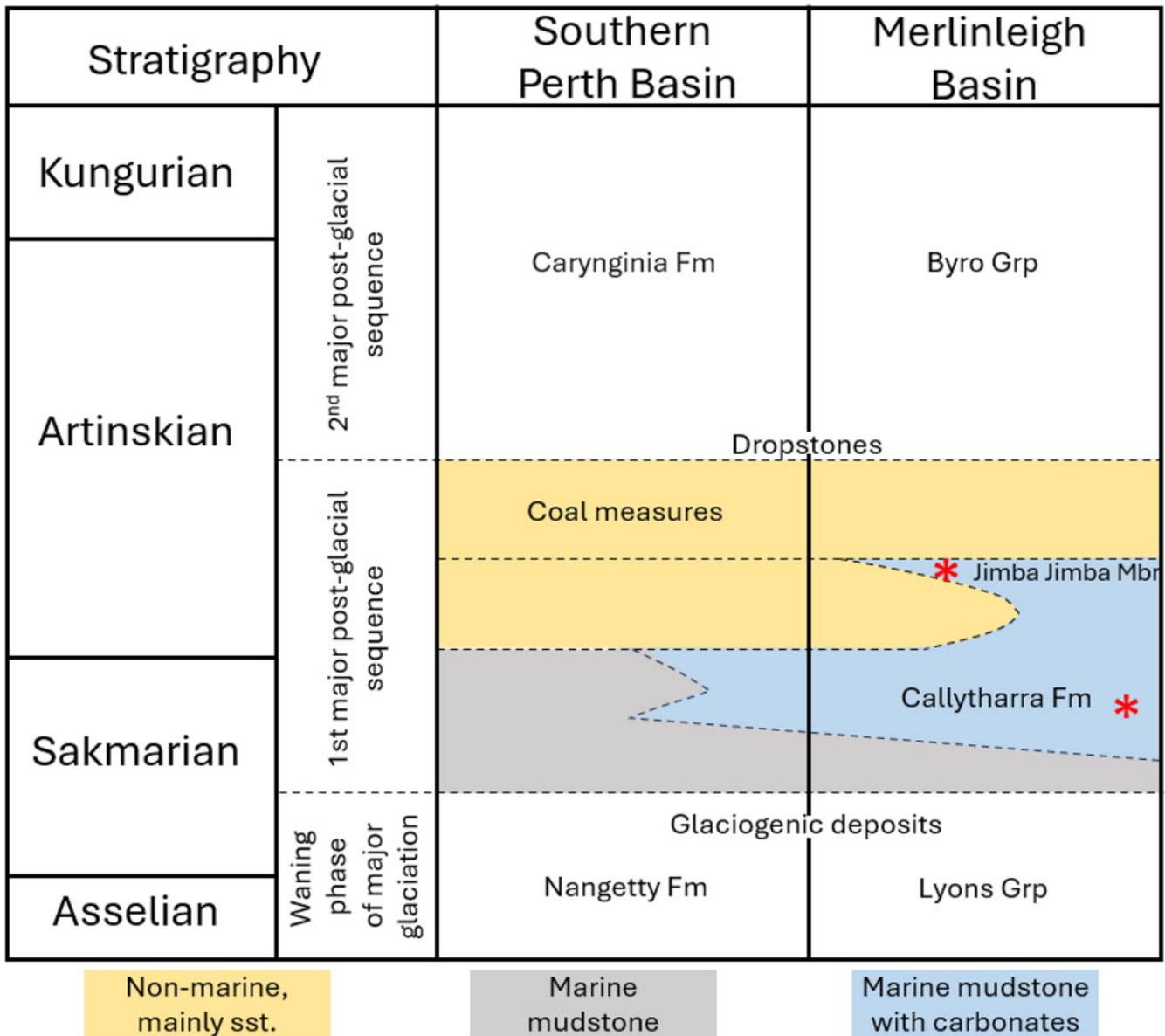
Figure 4. Sequence stratigraphy of the first major post-glacial sequence in the Merlinleigh and Southern Perth basins (simplified from Haig et al., 2014). The positions of the two *Evactinostella crucialis* (Hudleston, 1883) populations in this study are indicated by red asterisks.

Paleogeographically, they were deposited toward the southernmost marine strata in the East Gondwana Rift Zone at ~50°S paleolatitude (van Hinsbergen et al., 2015; Haig et al., 2017).

Tabulipora sp. is a trepostomate stenolaemate bryozoan (Taylor, 2020; Bock, 2023). Our specimens were originally assigned to *Amphiporella* (Madsen and Håkansson, 1989; Madsen, 1994). But since Boardman and Buttler's forthcoming Treatise on Invertebrate Paleontology (Part G, Bryozoa, Revised, Volume 2) subsumes *Amphiporella* into *Tabulipora* in keeping with Astrova's (1978) classification, we here refer to them as *Tabulipora* sp. Our species forms erect frondose colonies. The bifoliate, platy fronds are up to 1 cm thick, reaching over 20 cm wide (Madsen and Håkansson, 1989; Madsen, 1994). For this study, 15 colonies of *Tabulipora* sp. were selected from the series of samples collected from the Kim Fjelde Formation, Mallemuk Mountain Group, Wandel Sea Basin in North Greenland (Fig. 6) (Stemmerik and Håkansson, 1991; Watt, 2019). One

colony came from the Midnatfjeld section in eastern Peary Land at 82.7592°N, 22.1356°W, and 14 colonies came from the Kap Jungersen section in Amdrup Land 80.6283°N, 15.7489°W (Madsen, 1994) (Fig. 7). Specimen numbers and collection information are available in Table 2. Stratigraphically, these colonies lived during the Artinskian to Kungurian Ages of the Cisuralian Epoch of the Permian Period (Stemmerik et al., 1996, 2000; Henderson et al., 2020). Paleogeographically, they were deposited in the Wandel Sea Basin (Håkansson and Pedersen, 2015) at ~40°N paleolatitude (van Hinsbergen et al., 2015; Blakey, 2021, fig. 8).

Repository and institutional abbreviation. All specimens used in this study are deposited in the Western Australia Museum (WAM), Perth, Australia. Each specimen's WAM repository number is indicated in Table 1 or 2.
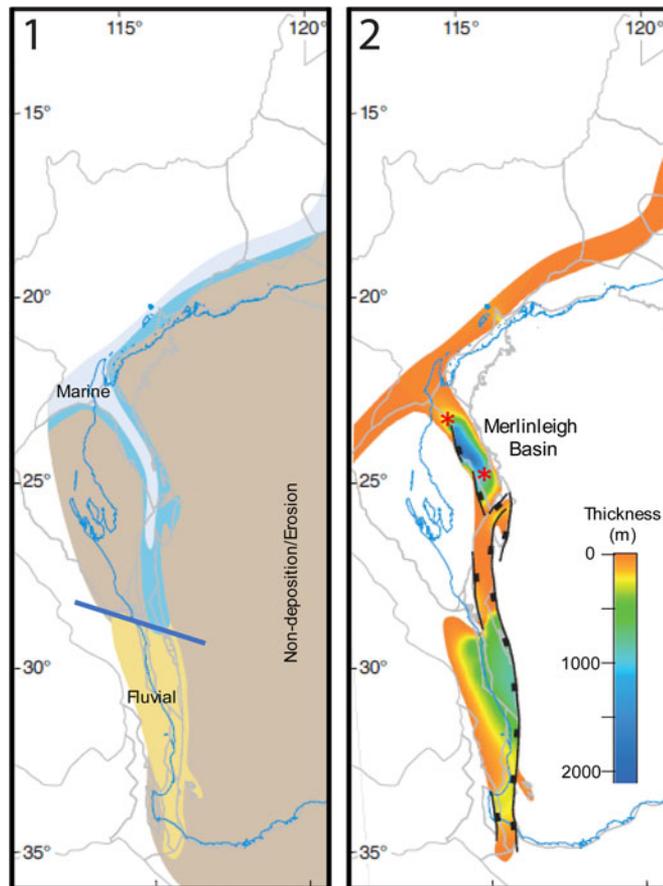
Figure 5. (**1**) Early Permian paleogeographic map of Western Australia. The main position of the fluctuating marine/terrestrial fluvial depositional boundary indicated by blue line. (**2**) Sediment isopach map relative to the positions of the two *Evactinostella crucialis* (Hudleston, 1883) populations investigated indicated by red asterisks: Lyndon River to the north and Jimba Jimba Station to the south. The distance between the two sample sites is approximately 220 km. Modified from Mory and Haines (2015, fig. 11a).

Methods

We measured branch width, branch thickness, and monticule height with digital calipers to the nearest 0.01 mm (Fig. 8). As discussed previously in Equation (3), curvature K was calculated as: $/K/ = \frac{b}{a^2}$ where a is the length of the semi-major axis (i.e., one-half branch width) and b is the length of the semi-minor axis (i.e., one-half branch thickness). Therefore, curvature in mm^{-1} as calculated in Equation (2) was $/K/ = \frac{\text{branch thickness}/2}{(\text{branch width}/2)^2}$. Monticule spatial density in number per mm^2 was calculated as the number of monticules per branch side/area of branch side. On some more weathered branches, monticules were not well enough preserved to be counted on both sides of the branch.

Using the structure-from-motion (SfM) method (Fonstad et al., 2013), we built digital elevation models (DEMs) of two branch surfaces. This is the first time SfM-DEM technology has been used in bryozoology. SfM applies the principles of stereoscopic photogrammetry to a series of two-dimensional digital images to reconstruct a three-dimensional DEM of the surface of an object (Westoby et al., 2012). For creating the DEMs, we chose one side of one branch from one colony from each species that had the largest surface area (i.e., the most monticules): WAM 2024.325C for *Tabulipora* sp. and WAM 2024.317A for *E.*

crucialis. The DEMs were built in Agisoft's Metashape Pro version 1.64 with 0.1 mm resolution on the x and y coordinate axes and 0.01 mm resolution on the z (vertical) axis. Topographic profiles through the colony surface were made with QGIS version 3.30 from monticule crest to monticule crest.

Results

The surfaces of the *Evactinostella crucialis* colonies (N = 17, curvature [mm^{-1}] range: 0.0021–0.0441, mean = 0.0118, standard deviation = 0.0104) are more curved than those of *Tabulipora* sp. (N = 15, curvature [mm^{-1}] range: 0.0012–0.0122, mean = 0.0063, standard deviation = 0.0032) (Tables 3, 4, respectively). On average, the more elliptical *Evactinostella* branches are significantly more (i.e., twice as) curved than those of the flatter *Tabulipora* branches (t-test two-sample assuming unequal variance: t-stat = 2.005, p = 0.059).

The caliper-based heights of the monticules on the *Evactinostella crucialis* colonies (N = 17, height [mm] range: 0.35–0.60, mean = 0.50, standard deviation = 0.08) are shorter than those on the *Tabulipora* sp. colonies (N = 10, height [mm] range: 0.40–1.85, mean = 1.10, standard deviation = 0.53) (Tables 3, 4, respectively). On average, monticules on the more elliptical *Evactinostella* branches are significantly shorter (i.e., half as high) than those of the flatter *Tabulipora* branches (t-test two-sample assuming unequal variance: t-stat = −3.364, p = 0.008).

The DEM-based monticule heights yielded similar results. The monticules on *Evactinostella crucialis* (N = 40, height [mm] range: 0.10–2.68, mean = 0.78, standard deviation = 0.47) are shorter than those on *Tabulipora* sp. (N = 31, height [mm] range: 0.89–2.40, mean = 1.48, standard deviation = 0.39). On average, monticules on the more elliptical *Evactinostella* branches are significantly shorter (i.e., half as high) than those of the flatter *Tabulipora* branches (t-test two-sample assuming unequal variance: t-stat = 6.761, p < 0.001) (Fig. 9).

Only among the *Evactinostella* colonies was branch surface curvature inversely proportional to monticule height as we expected (Fig. 10). The same was not true for the flatter *Tabulipora* sp. branches.

The monticules on the *Evactinostella crucialis* colonies (N = 16 colonies, spatial density [number/mm^2] range: 0.010–0.020, mean = 0.014, standard deviation = 0.003) are less densely spaced than those of *Tabulipora* sp. (N = 10, spatial density [number/mm^2] range: 0.016–0.025, mean = 0.018, standard deviation = 0.003) (Tables 3, 4, respectively). On average, the monticules on the more elliptical *Evactinostella* branches are significantly (i.e., 22%) less densely spaced as those of the flatter *Tabulipora* branches (t-test two-sample assuming unequal variance: t-stat = −3.746, p = 0.001).

Only among the *Evactinostella* colonies was branch surface curvature inversely proportional to monticule spatial density as we expected (Fig. 11). The same was not true for the flatter *Tabulipora* sp. branches.

Discussion

This study presumes that the monticules are sites of excurrent colony-wide feeding currents as previous authors have done (e.g., Yancey et al., 2019). Four independent pieces of evidence support this.

One: the monticules lack incurrent-generating feeding autozooids (Fig. 12). When an area of a colony surface is devoid of functioning autozooids with enough surrounding surface area of

Table 1. Sample, locality, and stratigraphic information for colonies of *Evactinostella crucialis* (Hudleston, 1883) used in this study from the Merlingleigh Subbasin at the southern end of the onshore Southern Carnarvon Basin, Western Australia.

| Western Australia Museum repository number	Collecting Institution	Collection date	Locality section	Lithostratigraphy
WAM 2024.317A	University of Western Australia	25 March 2011	NW of Jimba Jimba Station	Jimba Jimba Member, Callytharra Formation
WAM 2024.317B	University of Western Australia	25 March 2011	NW of Jimba Jimba Station	Jimba Jimba Member, Callytharra Formation
WAM 2024.317C	University of Western Australia	25 March 2011	NW of Jimba Jimba Station	Jimba Jimba Member, Callytharra Formation
WAM 2024.317D	University of Western Australia	25 March 2011	NW of Jimba Jimba Station	Jimba Jimba Member, Callytharra Formation
WAM 2024.318A	University of Western Australia	August 2014	Lyndon River	Callytharra Formation
WAM 2024.318B	University of Western Australia	August 2014	Lyndon River	Callytharra Formation
WAM 2024.318C	University of Western Australia	August 2014	Lyndon River	Callytharra Formation
WAM 2024.318D	University of Western Australia	August 2014	Lyndon River	Callytharra Formation
WAM 2024.318E	University of Western Australia	August 2014	Lyndon River	Callytharra Formation
WAM 2024.318F	University of Western Australia	August 2014	Lyndon River	Callytharra Formation
WAM 2024.318 G	University of Western Australia	August 2014	Lyndon River	Callytharra Formation
WAM 2024.318H	University of Western Australia	August 2014	Lyndon River	Callytharra Formation
WAM 2024.318I	University of Western Australia	August 2014	Lyndon River	Callytharra Formation
WAM 2024.318J	University of Western Australia	August 2014	Lyndon River	Callytharra Formation
WAM 2024.318K	University of Western Australia	August 2014	Lyndon River	Callytharra Formation
WAM 2024.318L	University of Western Australia	August 2014	Lyndon River	Callytharra Formation
WAM 2024.318M	University of Western Australia	August 2014	Lyndon River	Callytharra Formation
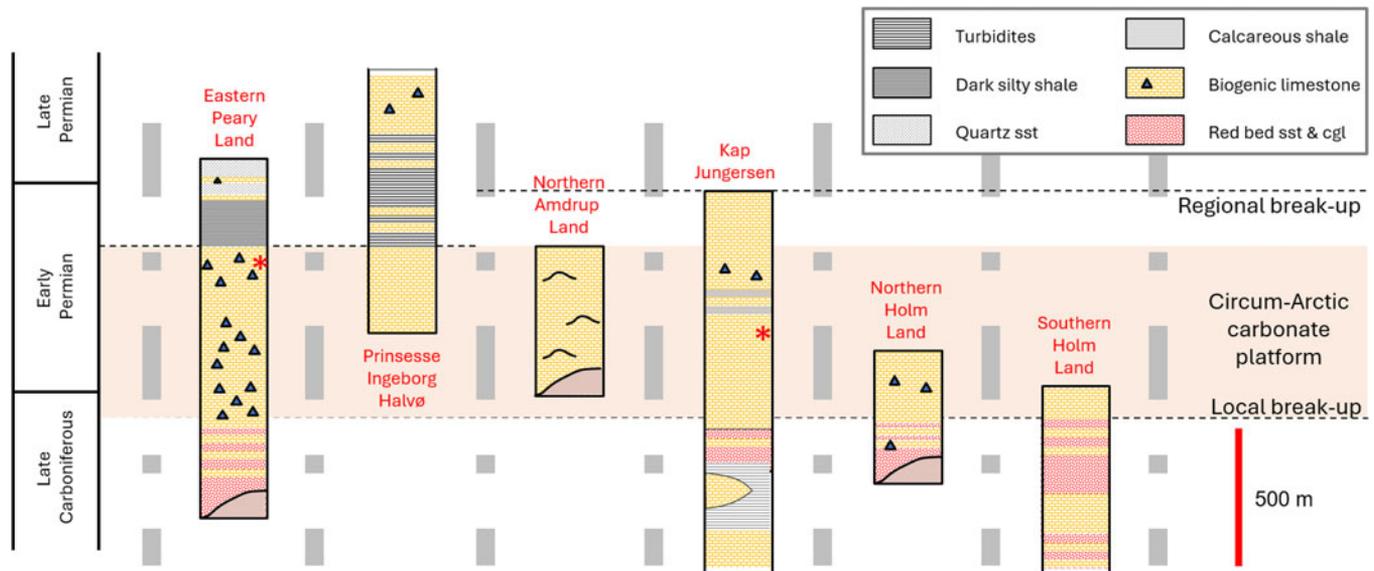
Figure 6. Stratigraphy of the late Carboniferous–early Permian Circum-Arctic carbonate platform segment in eastern North Greenland. Stylized fault blocks, created by transecting complex strike-slip fault system active intermittently from the Late Permian through the Mesozoic (Håkansson and Pedersen, 2015), are separated by gray dashed lines. The positions of the two populations of *Tabulipora* sp. in this study are indicated by red asterisks: Midnatfjeld section in eastern Peary Land and the Kap Jungersen section in Amdrup Land.

incurrent-generating autozooids, the devoid area by default becomes an excurrent chimney (Banta et al., 1974, fig. 1; McKinney, 1986a, fig. 4A; von Dassow, 2005a, fig. 1A). This study also assumes the monticules are the only sites of excurrent colony-wide feeding currents, and therefore, there are no non-skeletal chimneys interfering with our skeletal chimney interpretations. It is known that extant cheilostomes (e.g.,

Membranipora) can create excurrent chimneys simply by temporarily leaning their lophophores away from each other or retracting their polypides (Winston, 1978; Cook and Chimonides, 1980; Lidgard, 1981; Taylor, 1999; Shunatova and Ostrovsky, 2002). Fortunately, as shown by Shunatova and Ostrovsky (2002, table 1), such non-skeletal excurrent chimneys are not known from any stenolaemate bryozoans such as those in this study.

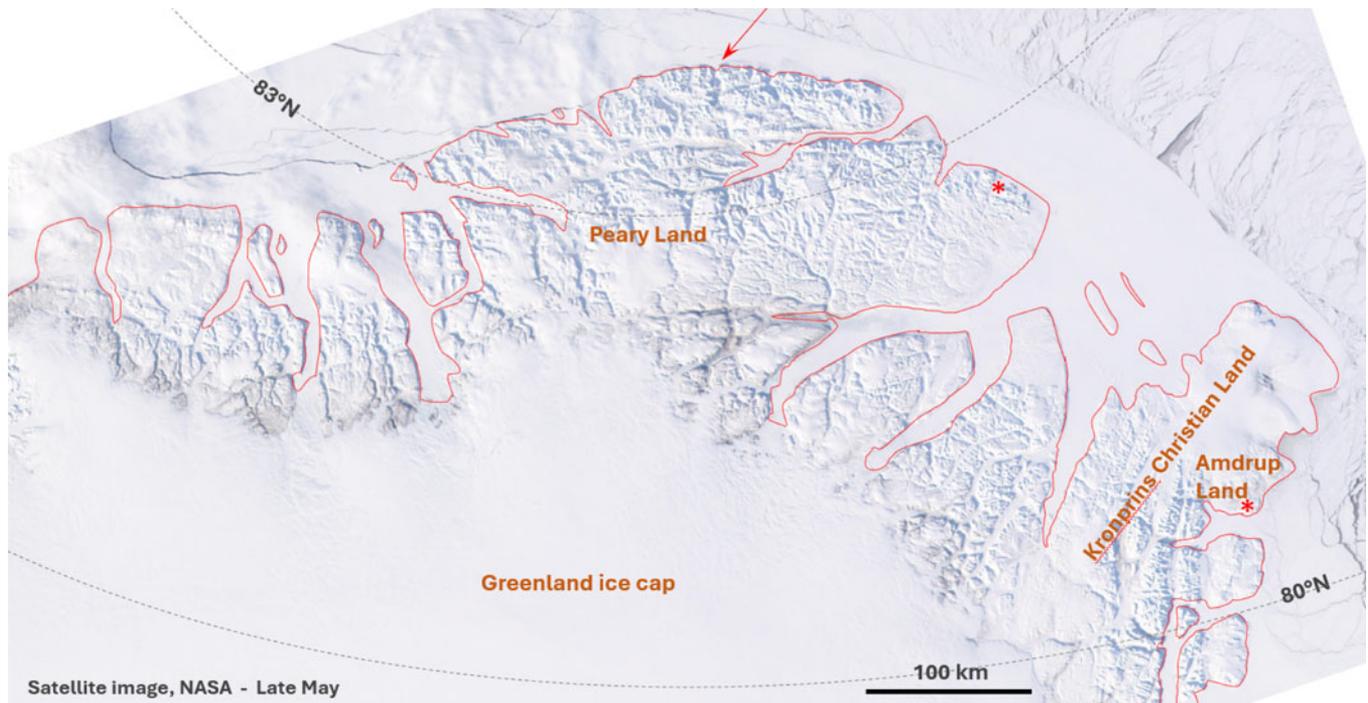**Figure 7.** This true-color Moderate Resolution Imaging Spectroradiometer (MODIS) satellite image from 20 May 2001 shows snow-covered North Greenland with the coastline indicated in red. The red arrow points to the northernmost point of land, and the position of the two populations of *Tabulipora* sp. investigated are indicated by red asterisks: Midnatfjeld to the north and Kap Jungersen to the south. Modified from Descloitres (2001).

Table 2. Sample, locality, and stratigraphic information for colonies of *Tabulipora* sp. used in this study from the Wandel Sea Basin in North Greenland.

| Western Australia Museum repository number	Collecting Institution	Collection date	Section	Region sensu Watt, 2019	Lithostratigraphy
WAM 20224.319	Geological Survey of Greenland	July 1978	Midnatfjeld	eastern Peary Land, North Greenland	Kim Fjelde Formation, Mallemuk Mountain Group, elevation ~437 m
WAM 20224.320	Geological Survey of Greenland	July 1980	Kap Jungersen	Amdrup Land, North Greenland	Kim Fjelde Formation, Mallemuk Mountain Group, 320–325 m above base of section
WAM 2024.321	Geological Survey of Greenland	July 1980	Kap Jungersen	Amdrup Land, North Greenland	Kim Fjelde Formation, Mallemuk Mountain Group, 325–330 m above base of section
WAM 2024.322A	Geological Survey of Greenland	July 1980	Kap Jungersen	Amdrup Land, North Greenland	Kim Fjelde Formation, Mallemuk Mountain Group, 335–345 m above base of section
WAM 2024.322B	Geological Survey of Greenland	July 1980	Kap Jungersen	Amdrup Land, North Greenland	Kim Fjelde Formation, Mallemuk Mountain Group, 335–345 m above base of section
WAM 2024.322C	Geological Survey of Greenland	July 1980	Kap Jungersen	Amdrup Land, North Greenland	Kim Fjelde Formation, Mallemuk Mountain Group, 335–345 m above base of section
WAM 2024.323A	Geological Survey of Greenland	July 1980	Kap Jungersen	Amdrup Land, North Greenland	Kim Fjelde Formation, Mallemuk Mountain Group, 366–375 m above base of section
WAM 2024.323B	Geological Survey of Greenland	July 1980	Kap Jungersen	Amdrup Land, North Greenland	Kim Fjelde Formation, Mallemuk Mountain Group, 266–275 m above base of section
WAM 20224.324A	Geological Survey of Greenland	July 1980	Kap Jungersen	Amdrup Land, North Greenland	Kim Fjelde Formation, Mallemuk Mountain Group, 385–395 m above base of section
WAM 2024.324B	Geological Survey of Greenland	July 1980	Kap Jungersen	Amdrup Land, North Greenland	Kim Fjelde Formation, Mallemuk Mountain Group, 385–395 m above base of section
WAM 2024.325A	Geological Survey of Greenland	July 1980	Kap Jungersen	Amdrup Land, North Greenland	Kim Fjelde Formation, Mallemuk Mountain Group, 395–405 m above base of section
WAM 2023.325B	Geological Survey of Greenland	July 1980	Kap Jungersen	Amdrup Land, North Greenland	Kim Fjelde Formation, Mallemuk Mountain Group, 395–405 m above base of section
WAM 2024.326A	Geological Survey of Greenland	July 1980	Kap Jungersen	Amdrup Land, North Greenland	Kim Fjelde Formation, Mallemuk Mountain Group, 403 m above base of section
WAM 2024.326B	Geological Survey of Greenland	July 1980	Kap Jungersen	Amdrup Land, North Greenland	Kim Fjelde Formation, Mallemuk Mountain Group, 403 m above base of section
WAM 2024.327	University of Copenhagen	July 1993	Kap Jungersen	Amdrup Land, North Greenland	Kim Fjelde Formation, Mallemuk Mountain Group, elevation ~326 m
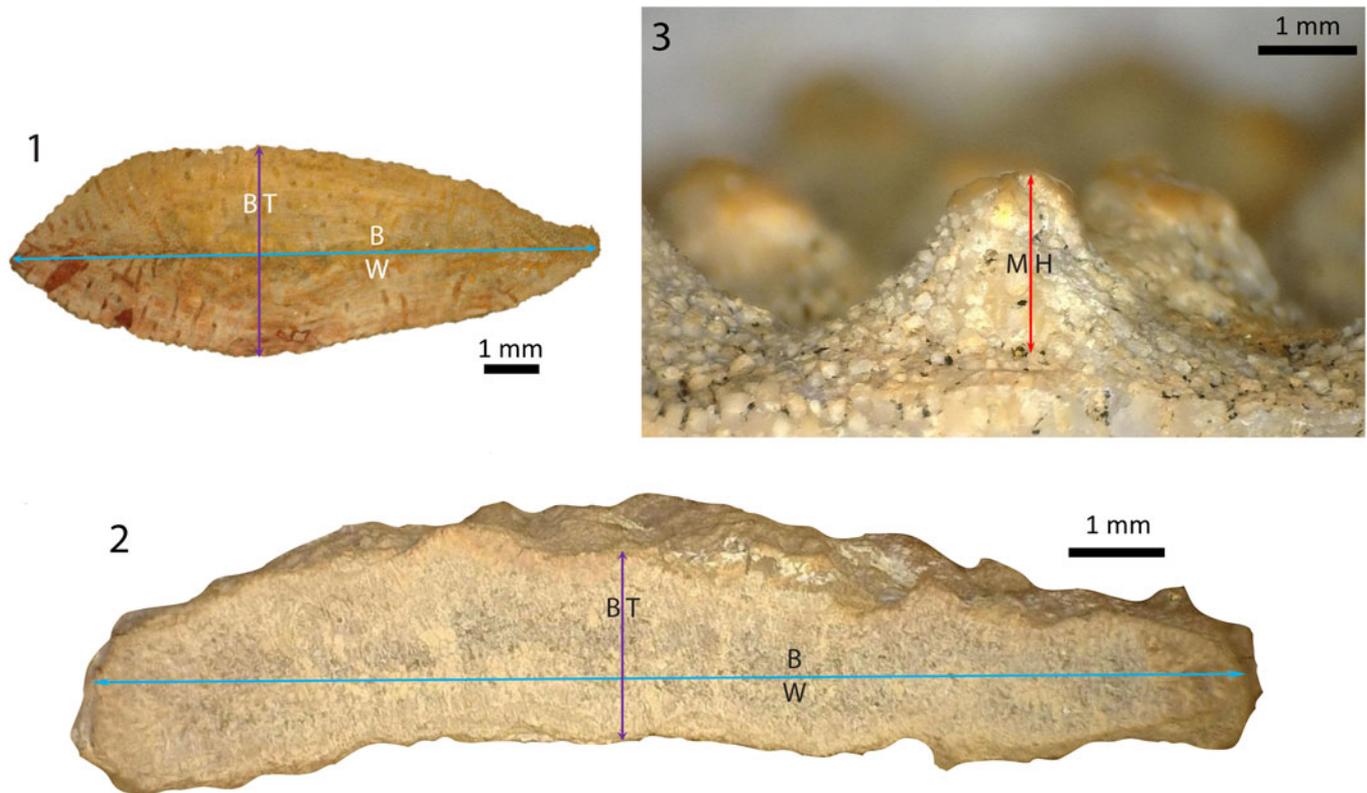
Figure 8. (**1, 2**) Caliper-based characters measured: branch thickness (BT) and branch width (BW) as shown on transverse cross-section views of (**1**) *Evactinostella crucialis* (Hudleston, 1883) specimen WAM 2024.317E from the Lyndon River locality in the Merlingleigh Subbasin at the southern end of the onshore Southern Carnarvon Basin, Western Australia, in the Callytharra Formation and (**2**) *Tabulipora* sp. specimen WAM 2024.326C from the Kap Jungersen locality in Amdrup Land, North Greenland, in the Kim Fjelde Formation, Mallemuk Mountain Group. (**3**) Monticule height (MH) as shown on a surface view of *Tabulipora* sp. specimen WAM 2024.325C from the Kap Jungersen locality in Amdrup Land, North Greenland, in the Kim Fjelde Formation, Mallemuk Mountain Group.

Two: the monticules have a stellate shape (Fig. 12) like other excurrent structures with centripetal flow. Many excurrent maculae are star-shaped (Anstey, 1987), for example, those in the cystoporate *Constellaria* (Boardman, 1983, fig. 59.1) and the trepostomes *Heterotrypa* (Anstey and Perry, 1973, pl. 17) and *Tabulipora* (Key et al., 2002, fig. 1). Key et al. (2011) used stream channel network analysis to show that stellate maculae in *Tabulipora* are excurrent chimneys. As first noticed by Anstey and Pachut (1976) and Anstey et al. (1976), stellate maculae are analogous to inorganic centripetal flow structures such as star dunes (e.g., Folk, 1971, fig. 5B; Nielson and Kocurek, 1987, fig. 2A) and araneiform CO_2 geysers on Mars (Portyankina et al., 2020, fig. 1). They are even more similar to centripetal flow structures in other organisms such as astrorhizae in living sclerosponges (e.g., Hartman and Goreau, 1970, fig. 5; Boyajian and LaBarbera, 1987, fig. 1) and fossil stromatoporoids (e.g., LaBarbera and Boyajian, 1991, fig. 1). The conical mamelons with radial bands in the Eocene demosponge *Pickettispongia tabelliformis* (Chapman and Crespin, 1934) from Australia illustrated by Pisera et al. (2023, fig. 5C) is a stunning example of evolutionary convergence with the monticules in this study.

Three: the autozooecial skeletal apertures are radially arranged around the centers of the monticules with the apertures facing away from the monticules (Fig. 12.1). Lunaria typically develop on the side of the aperture closest to the maculum (Anstey, 1981, 1987; Patzkowsky, 1987; Taylor, 1999). This is most evident in the cystoporate *Evactinostella crucialis* colonies that have

lunaria on the sides of autozooecial apertures nearest the centers of the monticules (Crockford, 1957; Utgaard, 1983). This makes the autozooecial apertures meet the colony surface very obliquely (Crockford, 1957) (Fig. 12.1). In extant colonies, this arrangement is associated with excurrent colony-wide feeding currents centered on maculae (Banta et al., 1974, fig. 1; Grünbaum, 1997, fig. 2a; von Dassow, 2005a, fig. 1B, 2005b, fig. 1B; Winston, 2010, fig. 2).

Four: the maculae are elevated (i.e., monticulate) (Figs. 8.3, 9). Most studies have attributed monticules to sites of excurrent flow (Banta et al., 1974, fig. 1; Taylor, 1999, fig. 41.3; Shunatova and Ostrovsky, 2002, fig. 7b; Winston, 2010, fig. 2; Taylor, 2020, fig. 4.22). However, not all monticules are centers of excurrent flow (Shunatova and Ostrovsky, 2002, fig. 7a).

Among the *Evactinostella* colonies, branch surface curvature was significantly inversely proportional to monticule height as we expected (Fig. 10). The same was true for the flatter *Tabulipora* sp. branches, but it was not significantly so (linear regression, $y = -22.644x + 1.2571$, $R^2 = 0.0176$, $p = 0.715$). We attribute this difference between *Evactinostella* and *Tabulipora* to less branch surface curvature in the latter. Flatter colonies (e.g., *Tabulipora*) will have a greater need to expel filtered water so should need higher monticules producing higher excurrent velocities. This is similar to star dunes where height is proportional to wind speed (Zhang et al., 2016).
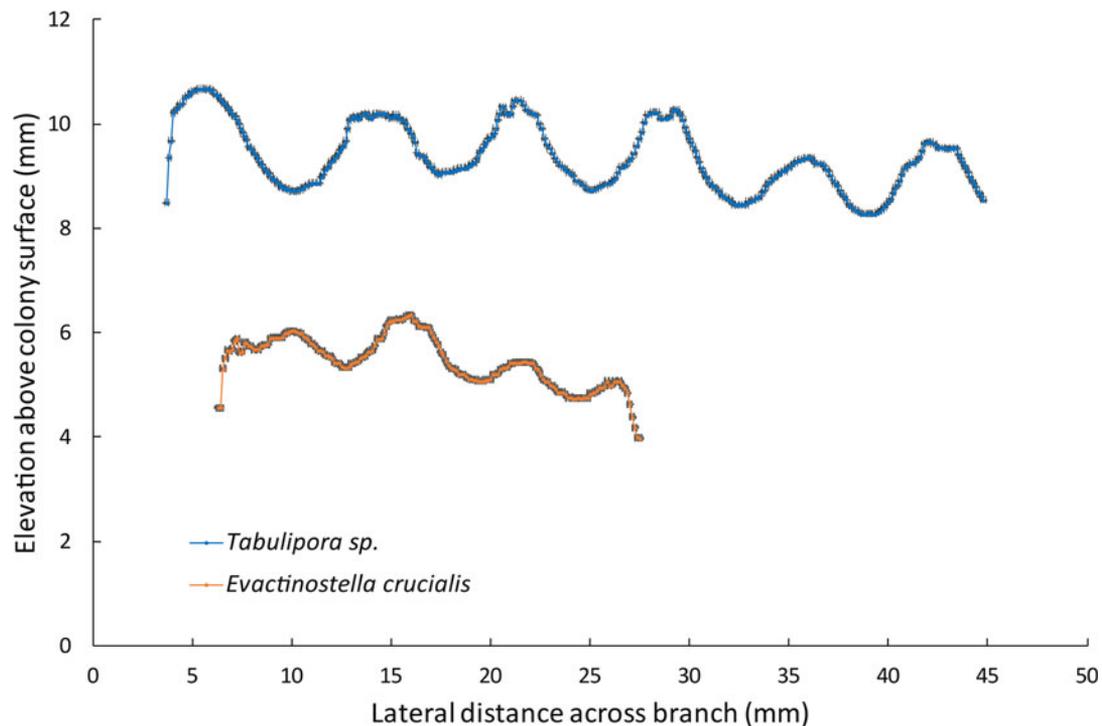
Among the *Evactinostella* colonies, branch surface curvature was inversely proportional to monticule spatial density as we

Table 3. Morphometric data for 17 colonies of *Evactinostella crucialis* (Hudleston, 1883) used in this study. Missing values are denoted by NA.

Western Australia Museum repository number of specimen	Branch dimensions						Monticule dimensions			
	Width (mm) perpendicular to branch axis at midpoint of branch	Thickness (mm) at midpoint along branch axis avoiding monticules	Thickness (mm) at midpoint along branch axis including monticules	Curvature (mm^{-1}) = (thickness/2)/((width/2)^2)	Branch surface area (mm^2) side 1	Branch surface area (mm^2) side 2	Mean monticule height (mm)	Number of monticules on side 1	Number of monticules on side 2	Number of monticules per mm^2 of branch surface area
WAM 2024.317A	26.3	3.4	4.2	0.0098	1,267	1,267	0.40	NA	NA	NA
WAM 2024.317B	49.0	4.1	5.2	0.0034	2,755	2,737	0.55	54	58	0.020
WAM 2024.317C	38.2	4.9	5.7	0.0067	1,984	1,979	0.40	31	32	0.016
WAM 2024.317D	33.3	4.0	5.2	0.0072	1,403	1,357	0.60	20	15	0.013
WAM 2024.318A	27.6	3.3	4.1	0.0087	566	989	0.40	6	15	0.014
WAM 2024.318B	29.2	3.2	4.3	0.0075	1,274	1,299	0.55	18	19	0.014
WAM 2024.318C	33.1	2.7	3.5	0.0049	1,231	1,279	0.40	20	19	0.016
WAM 2024.318D	60.4	3.8	4.8	0.0021	1,634	1,640	0.50	28	25	0.016
WAM 2024.318E	19.4	5.2	6.1	0.0276	1,297	1,329	0.45	17	19	0.014
WAM 2024.318F	24.4	5.7	6.8	0.0191	2,223	2,233	0.55	21	29	0.011
WAM 2024.318 G	23.2	4.3	5.5	0.0160	1,168	1,606	0.60	12	22	0.012
WAM 2024.318H	32.1	5.1	6.2	0.0099	1,416	1,445	0.55	20	15	0.012
WAM 2024.318I	27.4	2.3	3.4	0.0061	1,093	1,092	0.55	19	16	0.016
WAM 2024.318J	33.0	1.4	2.6	0.0026	1,026	1,071	0.60	16	14	0.014
WAM 2024.318K	23.4	1.8	2.8	0.0066	859	868	0.50	12	11	0.013
WAM 2024.318L	15.2	5.1	5.8	0.0441	931	949	0.35	9	10	0.010
WAM 2024.318M	18.5	3.1	4.1	0.0181	768	768	0.50	8	7	0.010

Table 4. Morphometric data for 15 colonies of *Tabulipora* sp. used in this study. Missing values are denoted by NA.

Western Australia Museum repository number of specimen	Branch dimensions					Monticule dimensions		
	Width (mm) perpendicular to branch axis at midpoint of branch	Thickness (mm) at midpoint along branch axis avoiding monticules	Thickness (mm) at midpoint along branch axis including monticules	Curvature (mm^{-1}) = (thickness/2)/((width/2)^2)	Branch surface area (mm^2) side 1	Mean monticule height (mm)	Number of monticules on side 1	Number of monticules per mm^2 of branch surface area
WAM 20224.319	123.7	9.0	9.0	0.0012	NA	NA	NA	NA
WAM 20224.320	60.7	10.1	10.1	0.0055	NA	NA	NA	NA
WAM 2024.321	44.2	9.1	9.1	0.0093	NA	NA	NA	NA
WAM 2024.322A	51.7	9.5	9.5	0.0071	NA	NA	NA	NA
WAM 2024.322B	71.5	4.9	4.9	0.0019	NA	NA	NA	NA
WAM 2024.322C	66.0	14.2	16.1	0.0065	4,589	0.95	75	0.016
WAM 2024.323A	81.4	5.8	6.6	0.0018	4,456	0.40	73	0.016
WAM 2024.323B	32.2	6.0	6.9	0.0116	2,461	0.45	40	0.016
WAM 20224.324A	30.8	4.3	6.2	0.0091	1,723	0.95	29	0.017
WAM 2024.324B	28.6	5.0	8.1	0.0122	1,364	1.55	27	0.020
WAM 2024.325A	35.8	4.4	6.0	0.0069	2,691	0.80	45	0.017
WAM 2023.325B	44.8	4.9	8.2	0.0049	2,702	1.65	46	0.017
WAM 2024.326A	46.0	4.2	7.9	0.0040	2,714	1.85	44	0.016
WAM 2024.326B	37.6	5.3	6.5	0.0075	877	0.60	22	0.025
WAM 2024.327	37.9	3.6	7.2	0.0050	1,563	1.80	30	0.019

Figure 9. Graph showing relative elevations of monticules on the DEM topographic profile monticules peak to peak across colonies. Error bars are ±0.1 mm on the horizontal axis and ±0.01 mm on the vertical axis. *Evactinostella crucialis* (Hudleston, 1883) data from specimen WAM 2024.317A and *Tabulipora* sp. data from specimen WAM 2024.325C.
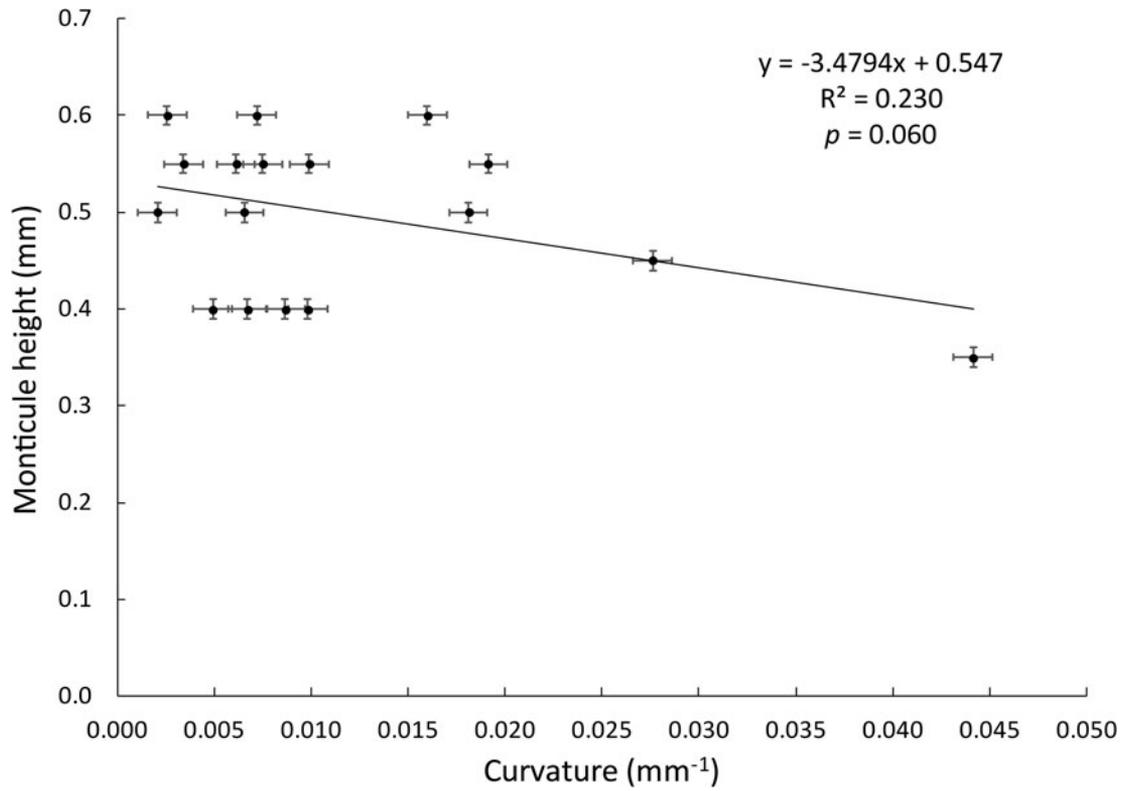
Figure 10. Graph showing inverse linear regression relationship between branch surface curvature and monticule height among the *Evactinostella crucialis* (Hudleston, 1883) colonies. Error bars are ±0.001 mm on the horizontal axis and ±0.01 mm on the vertical axis.
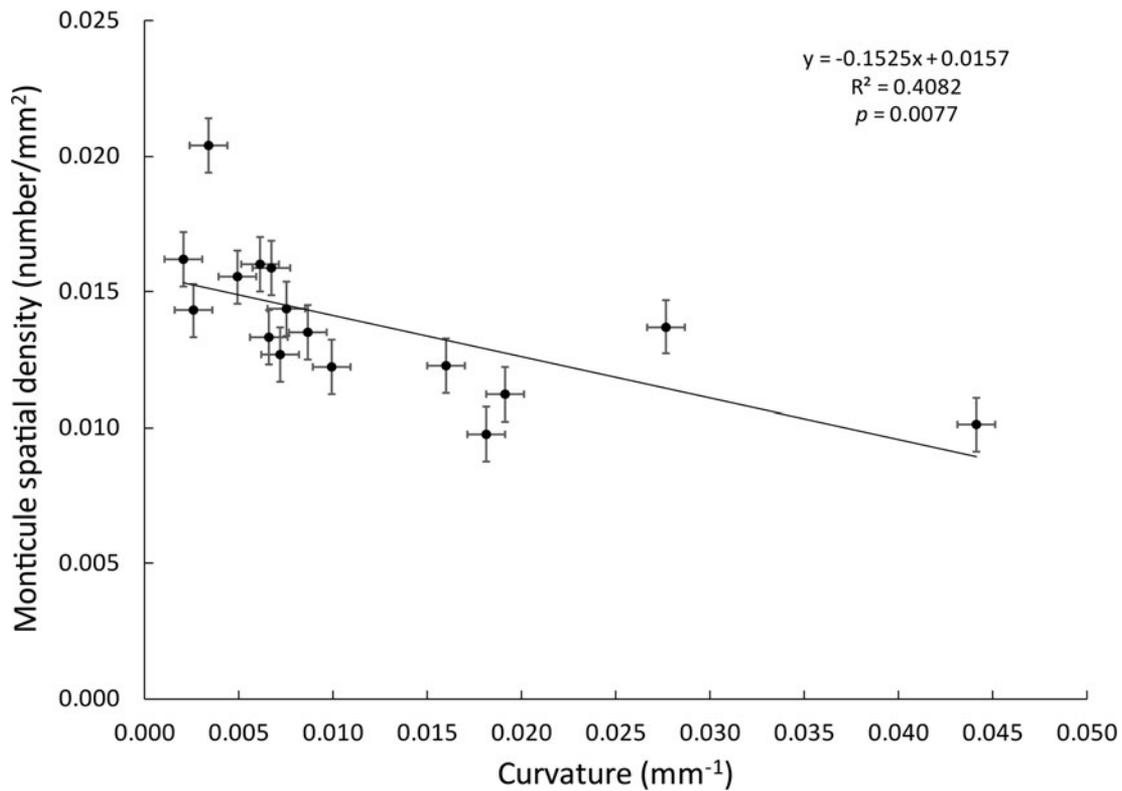

Figure 11. Graph showing inverse linear regression relationship between branch surface curvature and monticule spatial density among the *Evactinostella crucialis* (Hudleston, 1883) colonies. Error bars are ±0.001 mm.
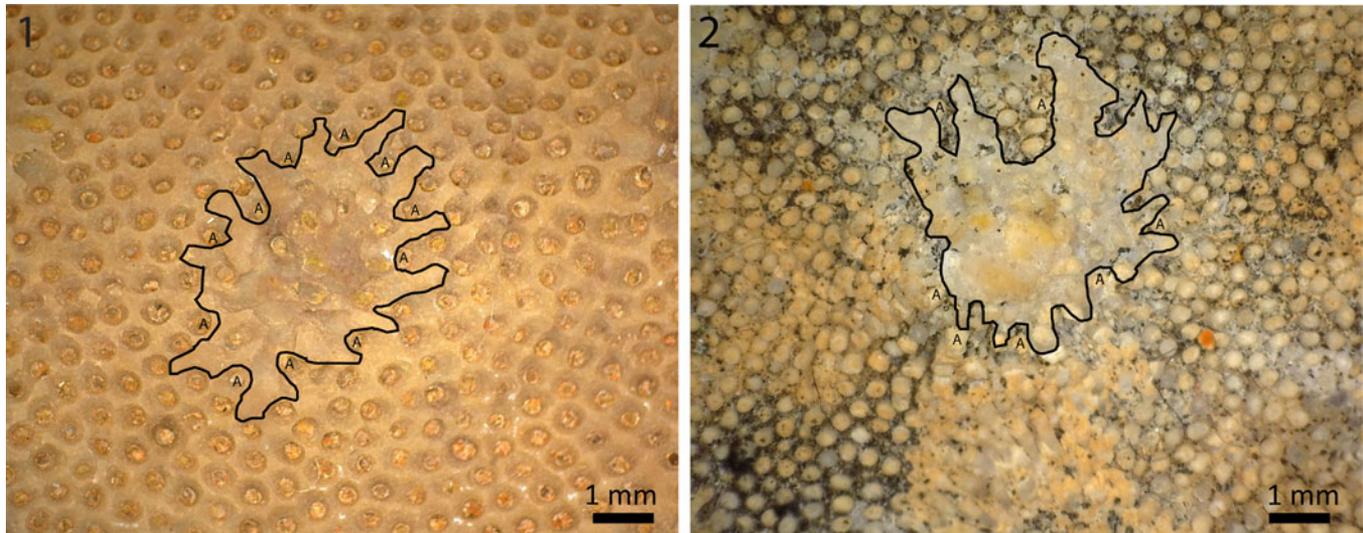
Figure 12. Plan view of outlined monticules in (**1**) *Evactinostella crucialis* (Hudleston, 1883) specimen WAM 2024.317E from the Jimba Jimba Station locality in the Jimba Jimba Member of the Callytharra Formation and (**2**) *Tabulipora* sp. specimen WAM 2024.326B from the Kap Jungersen locality in Amdrup Land, North Greenland, in the Kim Fjelde Formation, Mallemuk Mountain Group. Note lack of incurrent-generating feeding autozooids (A's), stellate shape, and autozooecial skeletal apertures facing away from the monticules.

expected (Fig. 11). The same was not true for the flatter *Tabulipora* sp. branches. We attribute this difference between *Evactinostella* and *Tabulipora* to less branch surface curvature in the latter. The magnitude of curvature in *Evactinostella* is more than twice as much as in *Tabulipora*, and the range is four times greater.

Alternatively, the weaker inverse correlation between branch surface curvature and monticule height and density in *Tabulipora* compared with *Evactinostella* may be a function of the former retaining a more constant branch cross-sectional shape through astogeny compared with *Evactinostella*, whose curvature changes more with colony age. This may not be the case as monticules have previously been correlated with bryozoan branch curvature. McKinney (1986b) measured 914 bryozoans with cylindrical branches and showed that macular chimneys form only in branches >2 mm diameter. Key et al. (2002) measured macular size in ramose *Tabulipora* colonies. They showed that as branch diameter increases (i.e., substrate curvature decreases), macular size increases. Wyse Jackson et al. (2014) measured monticule size in trepostomes encrusting conical nautiloids. They showed that as cone diameter increases (i.e., substrate curvature decreases), monticule size increases. Therefore, we conclude that the smaller and more curved the surface of a stenolaemate colony, the less the colony needs robust colony-wide feeding currents created by closely spaced tall monticules. Larger and flatter plate-like colonies need more robust colony-wide feeding currents created by closely spaced tall monticules.

Competing interests. The authors declare none.

References

Anderson, M.J., ed., 2017, *Flamingos: Behavior, Biology, and Relationship with Humans*: New York, Nova Science Publishers, 378 p.

Anstey, R.L., 1981, Zooid orientation structures and water flow patterns in Paleozoic bryozoan colonies: *Lethaia*, v. 14, p. 287–302.

Anstey, R.L., 1987, Colony patterning and functional morphology of water flow in Paleozoic stenolaemate bryozoans, *in* Ross, J.R.P., ed., *Bryozoa: Present and Past*: Bellingham, Western Washington University, p. 1–8.

Anstey, R.L., and Pachut, J.F., 1976, Functional morphology of animal colonies by comparison to sand dune paradigms: *Geological Society of America Abstracts with Programs*, v. 8, p. 124–125.

Anstey, R.L., and Perry, T.G., 1973, *Eden Shale bryozoans—a numerical study*: Michigan State University Paleontological Series, v. 1, 80 p.

Anstey, R.L., Pachut, J.F., and Prezbindowski, D.R., 1976, Morphogenetic gradients in Paleozoic bryozoan colonies: *Paleobiology*, v. 2, p. 131–146.

Astrova, G.G., 1978, The history of development, system, and phylogeny of the Bryozoa: Order Trepostomata: *Trudy Paleontologicheskogo Instituta Akademii Nauk SSSR*, v. 169, 240 p.

Banta, W.C., McKinney, F.K., and Zimmer, R.L., 1974, Bryozoan monticules; excurrent water outlets?: *Science*, v. 185, p. 783–784.

Bidder, G.P., 1923, The relationship of the form of a sponge to its currents: *Quarterly Journal of Microscopical Science*, v. 67, p. 292–323.

Bishop, J.W., and Bahr, L.M., 1973, Effects of colony size on feeding by *Lophopodella carteri* (Hyatt), *in* Boardman, R.S., Cheetham, A.H., and Oliver, W.A., Jr., eds., *Animal Colonies: Development and Function Through Time*: Stroudsburg, Dowden, Hutchinson, and Ross, p. 433–437.

Blakey, R., 2021, Paleotectonic and paleogeographic history of the Arctic region: *Atlantic Geology*, v. 57, p. 7–39.

Boardman, R.S., 1983, General features of the Class Stenolaemata, *in* Boardman, R.S., Lutaud, G., Wood, T.S., Karklins, O.L., Utgaard, J., Cheetham, A.H., and Cook, P.L., eds., *Treatise on Invertebrate Paleontology, Part G, Bryozoa 1 Revised*: Boulder, Colorado, Geological Society of America (and University of Kansas Press), p. 49–137.

Bock, P., 2023, Recent and fossil Bryozoa. https://www.bryozoa.net/trepostomatida/stenoporidae/index.html (accessed Aug 2023).

Boyajian, G.E., and LaBarbera, M.C., 1987, Biomechanical analysis of passive flow of stromatoporoids—morphologic, paleoecologic, and systematic implications: *Lethaia*, v. 20, p. 223–229.

Chapman, F., and Crespin, I., 1934, The palaeontology of the Plantagenet Beds of Western Australia: *Journal and Proceedings of the Royal Society of Western Australia*, v. 20, p. 103–136.

Colman, J.G., 1997, A review of the biology and ecology of the whale shark: *Journal of Fish Biology*, v. **51**, p. 1219–1234.

Cook, P.L., 1977, Colony-wide water currents in living Bryozoa: *Cahiers de Biologie Marine*, v. **18**, p. 31–47.

Cook, P.L., and Chimonides, P.J., 1980, Further observations on water current patterns in living Bryozoa: *Cahiers de Biologie Marine*, v. **21**, p. 393–402.

Crockford, J.M., 1957, *Permian Bryozoa from the Fitzroy Basin, Western Australia*: Bureau of Mineral Resources, Geology and Geophysics, Australia, Bulletin 34, 134 p.

Cuffey, R.J., and Fine, R.L., 2006, Reassembled trepostomes and the search for the largest bryozoan colonies: *International Bryozoology Association Bulletin*, v. **2**, p. 13–15.

Descloitres, J., 2001, *Northern coast of Greenland. MODIS Land Rapid Response Team, NASA/GSFC*: Visible Earth, NGreenland.A2001140.2015.250m.jpg.

Dick, M.H., 1987, A proposed mechanism for chimney formation in encrusting bryozoan colonies, *in* Ross, J.R.P., ed., *Bryozoa: Present and Past*: Bellingham, Western Washington University, p. 73–80.

d'Orbigny, A.D., 1850, *Prodrome de Paléontologie Stratigraphique Universelle des Animaux Mollusques et Rayonnés Faisant Suite au Cours Élémentaire de Paléontologie et Géologie Stratigraphiques*, Volume 2: Paris, Masson, 427 p.

Eckman, J.E., and Okamura, B., 1998, A model of particle capture by bryozoans in turbulent flow: *significance of colony form: American Naturalist*, v. **152**, p. 861–880.

Folk, R.L., 1971, Genesis of longitudinal and oghurd dunes elucidated by rolling upon grease: *Geological Society of America Bulletin*, v. **82**, p. 3461–3468.

Fonstad, M.A., Dietrich, J.T., Courville, B.C., Jensen, J.L., and Carbonneau, P.E., 2013, Topographic structure from motion: a new development in photogrammetric measurement: *Earth Surface Processes and Landforms*, v. **38**, p. 421–430.

Grünbaum, D., 1995, A model of feeding currents in encrusting bryozoans shows interference between zooids within a colony: *Journal of Theoretical Biology*, v. **174**, p. 409–425.

Grünbaum, D., 1997, Hydromechanical mechanisms of colony organization and cost of defense in an encrusting bryozoan, *Membranipora membranacea*: *Limnology and Oceanography*, v. **42**, p. 741–752.

Haig, D.W., McCartain, E., Mory, A.J., Borges, G., Davydov, V., et al., 2014, Postglacial early Permian (late Sakmarian–early Artinskian) shallow-marine carbonate deposition along a 2000 km transect from Timor to west Australia: *Palaeogeography, Palaeoclimatology, Palaeoecology*, v. **409**, p. 180–204.

Haig, D.W., Mory, A.J., McCartain, E., Backhouse, J., Håkansson, E., et al., 2017, Late Artinskian–early Kungurian (early Permian) warming and maximum marine flooding in the East Gondwana interior rift, Timor and Western Australia, and comparisons across East Gondwana: *Palaeogeography, Palaeoclimatology, Palaeoecology*, v. **468**, p. 88–121.

Håkansson, E., and Pedersen, S.A.S., 2015, A healed strike-slip plate boundary in North Greenland indicated through associated pull-apart basins, *in* Gibson, G.M., Roure, F., and Manatschal, G., eds., *Sedimentary Basins and Crustal Processes at Continental Margins: From Modern Hyper-Extended Margins to Deformed Ancient Analogues*: Geological Society of London Special Publication, v. **413**, p. 143–169.

Håkansson, E., Key, M.M., and Ernst, A., 2016, *Evactinostella* & *Lyroporella*—weird and wonderful bryozoans from Western Australia: 17th Conference of the International Bryozoology Association, Melbourne, Australia, Program and Abstracts, p. 49.

Hartman, W.D., and Goreau, T.F., 1970, Jamaican coralline sponges: their morphology, ecology and fossil relatives: *Symposia of the Zoological Society of London*, v. **25**, p. 205–243.

Henderson, C.M., Shen, S.Z., Gradstein, F.M., and Agterberg, F.P., 2020, The Permian Period, *in* Gradstein, F.M., Ogg, J.G., Schmitz, M.D., and Ogg, G.M., eds., *Geologic Time Scale 2020: Amsterdam*, Elsevier, p. 875–902.

Hentschel, B.T., and Shimeta, J., 2008, Suspension feeders, *in* Jørgensen, S.E., and Fath, B.D., eds., *Encyclopedia of Ecology: Cambridge*, Massachusetts, Academic Press, p. 3437–3442.

Hudleston, W.H., 1883, Notes on a collection of fossils and rock specimens from west Australia, north of the Gascoyne River: *Quarterly Journal of the Geological Society of London*, v. **39**, p. 582–595.

Key, M.M., Jr., Thrane, L., and Collins, J.A., 2002, Functional morphology of maculae in a giant ramose bryozoan from the Permian of Greenland, *in* Wyse Jackson, P.N., Buttler, C.J., and Spencer Jones, M.E., eds., *Bryozoan Studies 2001: Lisse*, the Netherlands, Balkema, p. 163–170.

Key, M.M., Jr., Wyse Jackson, P.N., and Vitiello, L.J., 2011, Stream channel network analysis applied to colony-wide feeding structures in a Permian bryozoan from Greenland: *Paleobiology*, v. **37**, p. 287–302.

LaBarbera, M.C., and Boyajian, G.E., 1991, The function of astrorhizae in stromatoporoids: *quantitative tests: Paleobiology*, v. **17**, p. 121–132.

Lebedeva, M.I., Sak, P.B., and Brantley, S.L., 2015, Using a mathematical model of a weathering clast to explore the effects of curvature on weathering: *Chemical Geology*, v. **404**, p. 88–99.

Lidgard, S., 1981, Water flow, feeding, and colony form in an encrusting cheilostome, *in* Larwood, G.P., and Nielsen, G., eds., *Living and Fossil Bryozoa: Fredensborg*, Denmark, Olsen and Olsen, p. 135–142.

Madsen, L., 1994, Bryozoans from the upper Palaeozoic sequence in the Wandel Sea Basin, North Greenland: *Wandel Sea Basin Analysis Scientific Report*, v. **6**, 18 p.

Madsen, L., and Håkansson., E., 1989, Upper Palaeozoic bryozoans from the Wandel Sea Basin, North Greenland: *Rapport Grønlands Geologiske Undersøgelse*, v. **144**, p. 43–52.

McKinney, F.K., 1986a, Evolution of erect marine bryozoan faunas: repeated success of unilaminate species: *American Naturalist*, v. **128**, p. 795–809.

McKinney, F.K., 1986b, Historical record of erect bryozoan growth forms: *Proceedings of the Royal Society of London*, v. **B228**, p. 133–148.

Mory, A.J., and Haines, P.W., 2015, A Paleozoic perspective of Western Australia, *in* Moss, S.J., and Keep, M., eds., *West Australian Basins Symposium 2013: Perth, Petroleum Exploration Society of Australia*, p. 1–25.

Nielson, J., and Kocurek., G., 1987, Surface processes, deposits, and development of star dunes: Dumont dune field, California: *Geological Society of America Bulletin*, v. **99**, p. 177–186.

Okamura, B., and Partridge, J.C., 2009, Suspension feeding adaptations to extreme flow environments in a marine bryozoan: *Biological Bulletin*, v. **196**, p. 205–215.

Patzkowsky, M.E., 1987, Inferred water flow patterns in the fossil *Fistulipora* M'Coy (Cystoporata, Bryozoa), *in* Ross, J.R.P., ed., *Bryozoa: Present and Past*: Bellingham, Western Washington University, p. 213–219.

Pisera, A., Bitner, M.A., and Fromont, J., 2023, Eocene phymaraphiniid demosponges from south Western Australia: filling the gap: *Acta Palaeontologica Polonica*, v. **68**, p. 261–272.

Portyankina, G., Hansen, C.J., and Aye, K.-M., 2020, How Martian araneiforms get their shapes: morphological analysis and diffusion-limited aggregation model for polar surface erosion: *Icarus*, v. **342**, n. 113217, https://doi.org/10.1016/j.icarus.2019.02.032.

Pratt, M.C., 2004, Effect of zooid spacing on bryozoan feeding success: is competition or facilitation more important?: *Biological Bulletin*, v. **207**, p. 17–27.

Shunatova, N.N., and Ostrovsky, A.N., 2002, Group autozooidal behaviour and chimneys in marine bryozoans: *Marine Biology*, v. **140**, p. 503–518.

Stemmerik, L., and Håkansson., E., 1991, Carboniferous and Permian history of the Wandel Sea Basin, North Greenland: *Bulletin Grønlands Geologiske Undersøgelse*, v. **160**, p. 141–151.

Stemmerik, L., Håkansson, E., Madsen, L., Nilsson, I., Piasecki, S., Pinard, S., and Rasmussen., J.A., 1996, Stratigraphy and depositional evolution of the upper Palaeozoic sedimentary succession in eastern Peary Land, North Greenland: *Bulletin Grønlands Geologiske Undersøgelse*, v. **171**, p. 45–71.

Stemmerik, L., Larsen, B.D., and Dalhoff, F., 2000, Tectono-stratigraphic history of northern Amdrup Land, eastern North Greenland: implications for the northernmost East Greenland shelf: *Geology of Greenland Survey Bulletin*, v. **187**, p. 7–19.

Taylor, P.D., 1979, The inference of extrazooidal feeding currents in fossil bryozoan colonies: *Lethaia*, v. **12**, p. 47–56.

Taylor, P.D., 1999, Bryozoa, *in* E. Savazzi, ed., *Functional Morphology of the Invertebrate Skeleton*: Chichester, Wiley, p. 623–646.

Taylor, P.D., 2020, *Bryozoan Paleobiology*; Hoboken, New Jersey, Wiley-Blackwell, 336 p.

Thorpe, J.P., and Ryland, J.S., 1987, Some theoretical limitations on the arrangement of zooids in encrusting Bryozoa, *in* Ross, J.R.P., ed., *Bryozoa: Present and Past*: Bellingham, Western Washington University, p. 276–283.

Utgaard, J., 1983, Paleobiology and taxonomy of the order Cystoporata, *in* Boardman, R.S., Lutaud, G., Wood, T.S., Karklins, O.L., Utgaard, J., Cheetham, A.H., and Cook, P.L., eds., *Treatise on Invertebrate Paleontology, Part G, Bryozoa 1 Revised*. Boulder, Colorado, Geological Society of America (and University of Kansas Press), p. 327–357.

van Hinsbergen, D.J.J., de Groot, L.V., van Schaik, S.J., Spakman, W., Bijl, P.K., Sluijs, A., Langereis, C.G., and Brinkhuis, H., 2015, A paleolatitude calculator for paleoclimate studies: *PloS ONE*, v. **10**, n. e0126946, https://doi.org/10.1371/journal.pone.0126946.

Vogel, S., 1994, *Life in Moving Fluids: The Physical Biology of Flow (second edition)*: Princeton, New Jersey, Princeton University Press, 467 p.

von Dassow, M., 2005a, Flow and conduit formation in the external fluid-transport system of a suspension feeder: *Journal of Experimental Biology*, v. **208**, p. 2931–2938.

von Dassow, M., 2005b, Effects of ambient flow and injury on the morphology of a fluid transport system in a bryozoan: *Biological Bulletin*, v. **208**, p. 47–59.

Watt, W.S., 2019, *Stratigraphic Lexicon for Greenland*: Rosendahls, Denmark, Geological Survey of Denmark and Greenland, 327 p.

Westoby, M.J., Brasington, J., Glasser, N.F., Hambrey, M.J., and Reynolds, J.M., 2012, 'Structure-from-motion' photogrammetry: a low-cost, effective tool for geoscience applications: *Geomorphology*, v. **179**, p. 300–314.

Winston, J.E., 1978, Polypide morphology and feeding behavior in marine ectoprocts: *Bulletin of Marine Science*, v. **28**, p. 1–31.

Winston, J.E., 1979, Current-related morphology and behavior in some Pacific coast bryozoans, *in* Larwood, G.P., and Abbott, M.B., eds., *Advances in Bryozoology*: London, Academic Press, p. 247–267.

Winston, J.E., 2010, Life in the colonies: learning the alien ways of colonial organisms: *Integrative and Comparative Biology*, v. **50**, p. 919–933.

Winston, J.E., and Migotto, A.E., 2021, Behavior, *in* Schwaha, T., ed., *Phylum Bryozoa*: Berlin, De Gruyter, p. 143–188.

Wyse Jackson, P.N., Key, M.M., Jr., and Coakley, S.P., 2014, Epizoozoan trepostome bryozoans on nautiloids from the Upper Ordovician (Katian) of the Cincinnati Arch region, USA: an assessment of growth, form, and water flow dynamics: *Journal of Paleontology*, v. **88**, p. 475–487.

Yancey, T.E., Wyse Jackson, P.N., Sutton, B.G., and Gottfried, R.J., 2019, Evactinoporidae, a new family of Cystoporata (Bryozoa) from the Mississippian of North America: growth and functional morphology: *Journal of Paleontology*, v. **93**, p. 1058–1074.

Zhang, W., Qu, J., Tan, L., Jing, Z., Bian, K., and Niu, Q., 2016, Environmental dynamics of a star dune: *Geomorphology*, v. **273**, p. 28–38.